Rate capability and magnetic field tolerance measurements of fast timing microchannel plate photodetectors

Junqi Xie[a,*], Mohammad Hattawy[a], Mickey Chiu[b], Edward May[a], Jose Repond[a], Robert Wagner[a], Lei Xia[a]

[a]*Argonne National Laboratory, Argonne IL 60439, USA*
[b]*Brookhaven National Laboratory, 2 Center St., Upton, NY, 11973, USA*

Abstract

Microchannel plate photodetectors provide both picosecond time resolution and sub-millimeter position resolution, they are attractive sensors for particle identification detectors of future US Electron Ion Collider. We have tested the rate capability and magnetic field tolerance of $6{\times}6$ cm^2 microchannel plate photodetectors fabricated at Argonne National Laboratory. The microchannel plate photodetector is designed of low-cost all-glass vacuum package with a chevron pair stack of "next generation" microchannel plates functionalized by atomic layer deposition. The rate capability test was performed with Fermilab 120 GeV primary proton beam, and the magnetic field tolerance test was performed on a solenoid magnetic facility with tunable magnetic field strength up to 4 Tesla. The gain of measured microchannel plate photodetector is stable up to 75 kHz/cm^2, and varies depending on the applied magnetic field strength and rotation angle relative to the magnetic field direction.

Index terms— Fast timing, Microchannel plate, Photodetector, Electron Ion Collider, Particle identification detector, Rate capability, Magnetic field, Rotation angle

1. Introduction

The Electron Ion Collider (EIC) [1] has been recommended in the 2015 Long Range Plan for Nuclear Science [2] as the highest priority for a new facility construction, with the mapping of the gluon content of nucleons and nuclei as the central goal. Several detector concepts are proposed and designed at Argonne National Laboratory (ANL), Brookhaven National Laboratory (BNL), Thomas Jefferson National Accelerator Facility (JLab) and some other institutes, with slightly different layout. For all these EIC detector designs, excellent particle identification (PID), especially hadron ($\pi/K/p$) separations over a wide range of momentum, is essential for the detailed measurements of several processes, such as the semi-inclusive deep inelastic scattering processes. Time-of-flight systems and imaging Cerenkov detectors (RICH, DIRC) [3, 4, 5] are proposed and studied, calling for large area, low cost photon sensors with high spatial resolution, high rate capability, radiation tolerance, magnetic field tolerance and picosecond timing resolution.

Microchannel plate (MCP) photodetectors are compact photon sensors, usually with an internal chevron pair stack of MCPs, providing both high spatial and temporal resolution in a vacuum package. The Large Area Picosecond Photodetector (LAPPDTM) is the world largest MCP based photodetector with an active area of $20{\times}20$ cm^2 [6]. It is designed of a modular all-glass detector package with the "next generation" MCPs produced by applying resistive and emissive coatings to borosilicate glass capillary array (GCA) substrates through atomic layer deposition (ALD) process. The all-glass design and low-cost "next generation" MCPs provide great advantages to reduce the LAPPDTM product cost per area compared to other MCP based photodetectors currently available. As a collaborator of the LAPPD project [7], we have built a MCP photodetector fabrication system [8] at Argonne National Laboratory to fabricate $6{\times}6$ cm^2 MCP photodetectors with LAPPD design. The fabricated MCP photodetectors were provided to several experiments for early test and adaption of LAPPD detector. The MCP photodetector fabrication system also serves as a R&D platform for LAPPD package design validation and optimization. Several $6{\times}6$ cm^2 MCP photodetectors with standard LAPPD design were successfully fabricated and tested [9, 10, 10], exhibiting high gain over 10^7, overall time resolution of 35 ps and position resolution better than 1 mm. The excellent performance of these $6{\times}6$ cm^2 MCP photodetectors shows that the low-cost LAPPDTM detector is a promising candidate for EIC PID photo sensors. Performance tests of the MCP photodetectors in high rate, high radiation damage and high magnetic field environments are required to further validate the application of LAPPDTM detectors as EIC PID photo sensors.

In this paper, we describe the current design of $6{\times}6$ cm^2 MCP photodetectors fabricated at Argonne National Laboratory, report recent results on the performance tests of these $6{\times}6$ cm^2 MCP photodetectors in high rate environment and high magnetic field environment. The direc-
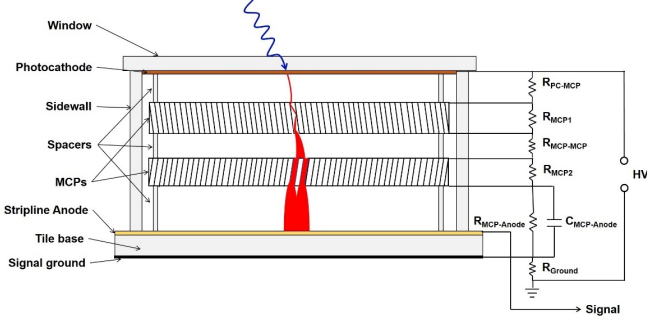
Figure 1: Schematic of MCP-based photodetector assembly (not to scale) and the electrical circuit diagram. External connections to the top and bottom surfaces of the two MCPs are through ultra-thin metal shims (not shown) to special extra strip lines on the tile base. The circuit diagram shows connections through side wall in a simplified format.
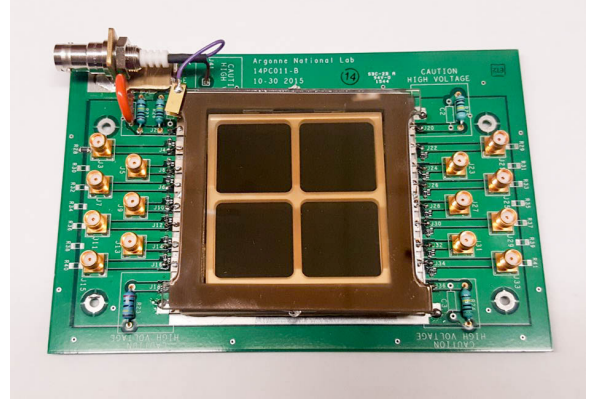

Figure 2: Completed MCP-based photodetector attached to a circuit board, providing firm electrical connections.

tion on further optimization of the LAPPDTM design for EIC PID application is also addressed at the end of this paper.

2. Design of the MCP-based photodetector assembly

Current design of the 6×6 cm^2 MCP photodetector is developed from the original LAPPD internal resistor chain design [11], similar to the current standard design of commercial LAPPDTM detectors [12]. Fig. 1 shows a schematic design (not to scale) of current MCP-based photodetector assembly and the electrical circuit diagram.

The MCP photodetector is an all glass body assembly, consists of glass base window, top window, side wall, three grid spacers and two MCPs. The sidewall is frit bonded onto the base window, with silver stripline anodes printed, leading the signals and high voltage connections to outside. Grid spacers are placed between anode and MCPs and top window as insulators to separate these components, they also hold these internal components in place in the vacuum assembly. Four ultra-thin metal shims are applied at the top and bottom surfaces of the two MCPs to lead the electrical connection to external connections, detailed circuit connection inside the vacuum package is described in reference [13]. This independent bias-voltage design provides advantage of individually controlling and fine tuning of the bias voltage for each MCP. Bialkali photocathode is deposited on the inside surface of the top window, and an indium seal is made between the top window and the sidewall through a low temperature thermo-compression sealing process to form a hermetic vacuum detector package. The completed MCP-based photodetector is attached to a custom-made circuit board, providing a permanent mount and firm electrical connections as shown in Fig. 2. External electrical connections for both signal and high voltage are co are inserted into the external resistor connections to serve as high voltage divider, ensuring both MCPs work at an independently optimized high voltage for best performance. Additional capacitors may also be added across the resistor divider for better signal waveform.

The microchannel plates used in the 6×6 cm^2 MCP photodetector are diced from the "next generation" large area (20×20 cm^2) MCPs [6, 12], the world largest commercially available MCPs. These "next generation" MCPs are produced through a glass drawing process and functionalized through atomic layer deposition, completely different from the production of traditional leaded glass MCPs. The glass drawing process uses borosilicate glass as tube materials, which is considerably less expensive than the leaded glass and eliminates the chemical etching process required in traditional method, making it much more cost-effective for MCP production. Here, we use standard borosilicate glass MCPs with 20 μm pore size, 60:1 L/d (pore length to diameter) ratio and 8o bias angle relative to the MCP surface normal. The two MCPs are placed as the "chevron" configuration in the vacuum package, which reversed the bias angle to -8°.

3. Rate capability measurement

The rate capability of MCP-based photodetectors is one of the most critical parameters for applications in high luminosity environment, such as EIC. Due to the high resistive layer coating on ALD functionalized MCPs, the current in the MCP pores may not flow off fast enough when the MCP-based detector is exposed to high particle rates. This effect may cause severe charge saturation, reduce the gain of the MCP-based photodetector and limit the detector performance.

We investigated the rate capability of the 6×6 cm^2 MCP-based photodetectors with 120 GeV/c primary proton beam at the Fermilab Test Beam Facility (FTBF). The beam was delivered as a slow spill with a 4 s duration once per minute with a maximum intensity of 10^5 particles per spill. The beam shape is circular with a diameter of 6 mm and a gaussian density profile. The beam intensity was close to a constant during each spill period. On
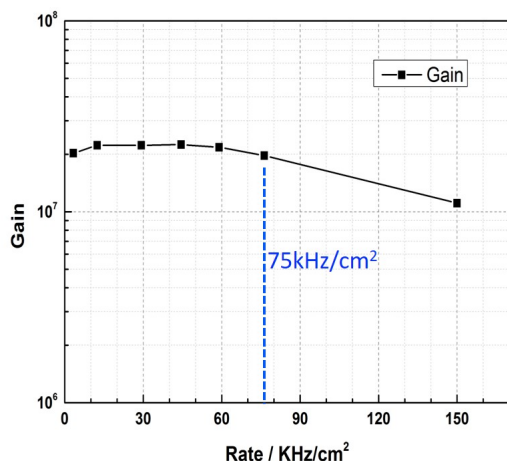
2

Figure 3: Gain of MCP-based photodetector as a function of the 120 GeV/c proton beam flux. The gain of the detector is stable up to beam flux of 75 kHz/cm^2, and the gain is still over 10^7 at 150 kHz/cm^2.
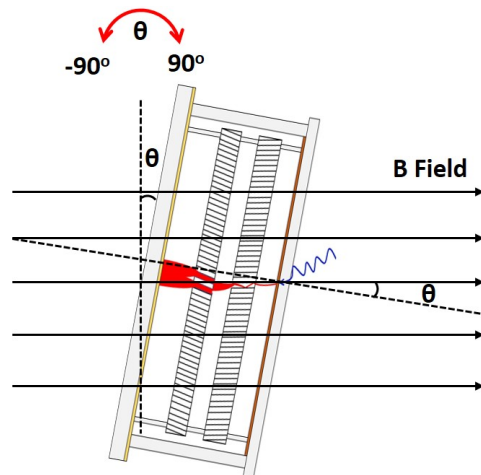

Figure 4: Schematic of the rotation of MCP-based photodetector with angle θ relative to the magnetic field direction during the measurement.

the beamline, the 120 GeV/c incident proton beam was monitored by an upstream multiwire proportional counter to see the beam profile. Three plastic scintillators in coincidence were used as a trigger and to count the number of incident proton. A light-tight dark box was designed to hold the MCP-based photodetector in the beam path with the detector surface facing the beam direction. High voltage was applied to the MCPs through external resistor voltage divider, and signals from the strip lines were readout through the DT5742 desktop digitizer [14] produced by CAEN (Costruzioni Apparecchiature Elettroniche Nucleari S.p.A.) with a sampling rate of 5 GS/s. The digitizer is based on the switched capacitor array DRS4 (Domino Ring Sampler) chip [15] and have 16 analog input channels and 1 additional analog input for fast trigger.

During our experiment, the 120 GeV/c proton beam intensity was tuned to vary from 500 to 40,000 particles per spill. The beam rate was calculated using the number of triggers per spill and was corrected for the size of the beam spot by reconstructing the beam profile. The calculated beam rate varies from 3 to 150 kHz/cm^2 corresponding to the monitored beam particle intensity. Fig. 3 shows the gain of the MCP-based photodetector measured as a function of the beam rate. The measured gain of the investigated detector is stable up to a beam flux of 75 kHz/cm^2 and still over 10^7 when the beam flux reaches 150 kHz/cm^2. Such a high rate capability of the MCP-based photodetector would be sufficient for EIC PID detectors, which are expected to work at a rate environment of xxx Hz/cm^2.

4. Magnetic field tolerance measurement

In the EIC detectors, solenoid magnet with field strength of 1.5 Tesla are proposed. The imaging erenkov detectors (RICH, DIRC) and time-of-flight systems are designed to cover the area of the barrel and end caps for charged particle ($\pi/K/p$) separations. This compact design requires the photo sensors working properly in a harsh environment with magnetic field strength up to 1.5 Tesla.

At Argonne National Laboratory, a decommissioned superconducting magnet from a magnetic resonance imaging (MRI) scanner was acquired to test instruments for the muon g-2 experiment [16]. The magnet provides a large bore with a diameter of 68 cm and a very homogenous field (7 ppb/cm), the magnitude of the magnetic field is tunable up to 4 Tesla. We have built a characterization system compatible with the solenoid magnet to test the performance of the 6×6 cm^2 MCP-based photodetector in strong magnetic field environment. The MCP photodetector was fixed in a custom built non-magnetic, light-tight dark box. The dark box was held on a test platform with the detector surface normal to the direction of magnetic field. The position of the dark box was adjusted so that the center of the MCP photodetector is well aligned with the center of the solenoid magnet. A rotation mechanism was also integrated with the system, allowing rotation of the MCP-based photodetector with angle θ as shown in Fig. 4 (not to scale). A 405 nm light-emitting diode (LED) was used as the light source and introduced to the surface of the MCP photodetector through an optical fiber. High voltage was applied to the MCPs from a supply with variable voltage control, and signals from the strip lines were readout through CAEN DT5742 desktop digitizer.

4.1. Magnetic field strength dependence

The dependence of the MCP photodetector performance on the magnetic field strength was done at rotation angle
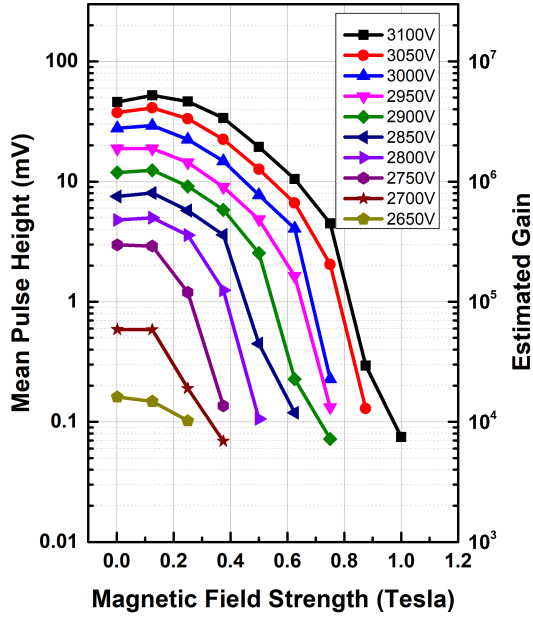
Figure 5: Dependence of the MCP-based photodetector gain on the magnetic field strength at different bias voltages.
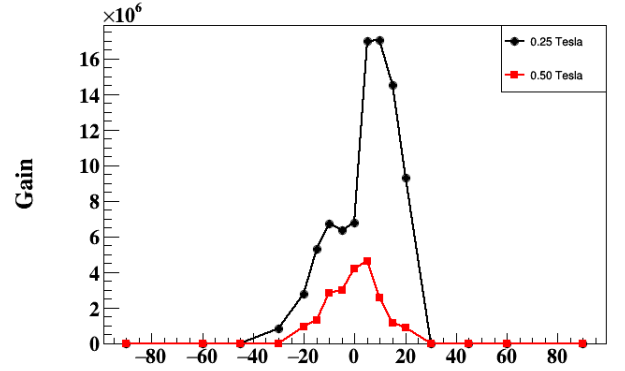

Figure 6: Gain of MCP-based photodetector as a function of rotation angle *theta* relative to the direction of magnetic field. The two peaks around -8° and 8° indicates the effect due to the 8° bias angle of the MCPs. Note that the intensities of these two peaks are not the same due to the different effect from top and bottom MCPs.

$\theta = 0°$, i.e., the direction of the magnetic field is normal to the surface of the MCP-based photodetector. We measured the gain of the investigated MCP photodetector in various magnetic field environment with different bias voltages, the results are plotted in Fig. 5. The gain is calculated based on integrated charge in pulse normalized to single photoelectron. At a fixed bias high voltage, the gain of MCP photodetector increases slightly as the magnetic field strength increases to 0.2 T, and starts to decrease as the magnetic field strength continues to increase, and eventually breaks down at magnetic field strength of 0.8 T. In the same magnetic field environment, the gain of the MCP photodetector increases as the biased high voltage increases. This behavior is similar to our previous measurement of the MCP photodetectors without applying magnetic field.

4.2. Magnetic field angle dependence

The performance of MCP-based photodetector at different angle was also studied by rotating the MCP photodetector along with angle θ relative to the magnetic field direction, as shown in Fig 5. We fixed the biased high voltage at 3000 V on the photodetector and rotated the photodetector from -90° to 90° for a full angle measurement. Fig. 6 shows the gain of MCP photodetector measured as a function of the rotation angle θ at magnetic field strength of 0.5 and 0.25 Tesla respectively. The MCP photodetector almost does not provide detectable signals when θ -30° or θ 30°. Within - 30° θ 30°, there are two gain peaks at $\theta = -8°$ and $\theta = 8°$, which is due to the "chevron" configuration of two MCPs inside the photodetector. The gain reaches a maximum when the pore of either MCP is

well aligned with the magnetic field direction. Meanwhile, the intensities of the two peaks are different, which is due to the different effect from the top and bottom MCPs.

4.3. Design optimization of MCP-based photodetector

In EIC experiment, 1.5 Tesla solenoid magnet will be used for tracking charged particles. The magnetic field tolerance requirement varies from detector to detector depending on their distance and direction to the magnet, and is up to 1.5 Tesla. From our measurement, the 6×6 cm^2 MCP-based photodetector has shown a good magnetic field tolerance up to 0.8 Tesla, comparable to that of current commercially available MCP-PMTs (1.0 T) with similar pore size [17]. Here, we must emphasize that the current LAPPD design is not optimized yet for magnetic field tolerant applications. The distances between the photocathode, MCPs and anode are pretty large in the LAPPD design, e.g., spacings between the photocathode and MCPs are 2 mm and the spacing between the MCP and anode is 3.2 mm [10], these distances should be reduced to minimize the electron transit distance. Meanwhile, MCP photodetectors with smaller pore size MCPs have shown better magnetic field tolerance than the ones with larger pore size MCPs [17, 18, 19]. A redesign of the current LAPPD configuration with smaller pore size (e.g.10 μm or even 5 μm) "next generation" MCPs and reduced distances between the PMT elements would further improve its magnetic field tolerance to the required level.

5. Conclusions

We have described the current design of 6×6 cm^2 microchannel plate photodetectors with "next generation" MCPs functionalized through atomic layer deposition process. The rate capability and magnetic field tolerance of

these photodetectors were tested at Fermilab 120 GeV proton beam and Argonne 4 Tesla magnetic field facility respectively. The photodetectors exhibit stable performance up to 75 kHz/cm^2 and magnetic field tolerance up to 0.8 Tesla. The magnetic field angle dependence was also measured, showing enhanced performance at $\pm 8°$ tilt angle due to the original MCP $8°$ bias angle. The magnetic field tolerance of these detectors should be further improved by applying smaller pore size MCPs and redesign the package with reduced distances between the photocathode, MCPs and anode.

6. Acknowledgments

References

[1] A. Accardi et al., Electron Ion Collider: The Next QCD Frontier, Eur. Phys. J. A 52 (2016) 268.

[2] A. Aprahamian et al., Reaching for the horizon: The 2015 long range plan for nuclear science, 2015.

[3] C.P. Wong et al., Modular focusing ring imaging Cherenkov detector for electron-ion collider experiments, Nucl. Instr. and Meth. A 871 (2017) 13.

[4] A. Del Dotto et al., Design and R&D of RICH detectors for EIC experiments, Nucl. Instr. and Meth. A (2017).

[5] G. Kalicy et al., High-performance DIRC detector for the future Electron Ion Collider experiment, JINST 11 (2016) C07015.

[6] M. Minot et al., Pilot production & commercialization of LAPPDTM, Nucl. Instr. and Meth. A 787 (2015) 78.

[7] B. Adams et al., A brief technical history of the Large-Area Picosecond Photodetector (LAPPD) Collaboration, 2016 arXiv:1603.01843.

[8] J. Xie et al., Development of a small form-factor (6cm×6 cm) picosecond photodetector as a path towards the commercialization of large area devices, in: Proceeding of "The Technology and Instrumentation in Particle Physics 2014", PoS 2014.

[9] J. Xie et al., Design and fabrication of prototype 6×6 cm^2 microchannel plate photodetector with bialkali photocathode for fast timing applications, Nucl. Instr. and Meth. A 784 (2015) 242.

[10] J. Wang et al., Development and testing of cost-effective, 6cm×6cm MCP-based photodetectors for fast timing applications, Nucl. Instr. and Meth. A 804 (2015) 84.

[11] J. Wang et al., Design improvement and bias voltage optimization of glass-body microchannel plate picosecond photodetector, IEEE Trans. Nucl. Sci. 64 (2017) 1871.

[12] C. Craven et al., Recent advances in Large Area Micro-Channel Plates and LAPPDTM, Springer Proceedings in Physics (2017).

[13] L. Xia et al., Systems and methods for forming microchannel plate (MCP) photodetector assemblies, U.S. Patent 9704900 B1, July 11, 2017.

[14] DT5742 desktop digitizer ¡ http://www.caen.it/jsp/Template2/CaenProd. ¿

[15] DRS chip developed at Paul Scherrer Institut, Switzerland ¡ https://www.psi.ch/drs ¿

[16] 4 Tesla Magnet Facility ¡ https://www.anl.gov/hep/group/4-tesla-magnet-facility ¿

[17] A. Lehmann et al., Performance studies of microchannel plate PMTs in high magnetic fields, Nucl. Instr. and Meth. A 595 (2008) 173.

[18] A. Lehmann et al., Systematic studies of micro-channel plate PMTs, Nucl. Instr. and Meth. A 639 (2011) 144.

[19] Y. Ilieva et al., MCP-PMT studies at the High-B test facility at Jefferson Lab, JINST 11 (2016) C03061.